Available online at www.sciencedirect.com
ScienceDirect
Information Fusion 9 (2008) 317–326
INFORMATION FUSION
www.elsevier.com/locate/inffus

Information driven localisation of a radiological point source

Branko Ristic *, Ajith Gunatilaka

Defence Science and Technology Organisation, 506 Lorimer Street, Fishermans Bend, VIC 3207, Australia

Received 25 August 2006; received in revised form 5 June 2007; accepted 21 June 2007
Available online 6 July 2007

Abstract

The paper presents an algorithm for detection and a subsequent information gain driven control of the observer for the purpose of parameter estimation of an unaccounted point source of relatively low-level gamma radiation. The source parameters to be estimated are its location and intensity. Source detection and parameter estimation are carried out jointly in the Bayesian framework using a particle filter. The observer motion and the radiation exposure time are controlled by the algorithm. Initially the observer control vectors take predefined values until the source is positively detected. After detection, the control vectors are selected sequentially for the purpose of reduction in the observation time and consequently the radiation exposure. The selection of control vectors is carried out via a multiple-step ahead maximisation of the Fisher information gain.
Crown Copyright © 2007 Published by Elsevier B.V. All rights reserved.

Keywords: Monte Carlo estimation; Resource allocation; Cramér–Rao bound; Radiological data fusion; Nuclear search

1. Introduction

Since the end of the Cold War, the risk of nuclear proliferation has increased dramatically due to the relative ease of acquiring radioactive materials [19]. Of growing concern is that numerous accidents have already been reported involving a loss or theft of radioactive sources, which could potentially be used to improvise nuclear devices for high-impact spectacular attacks [19]. A *dirty bomb*, for example, is a radiological weapon which consists of a conventional explosive packaged with radioactive materials, aimed to kill or injure through the initial blast of the conventional explosive and by airborne radiation and contamination.

This paper proposes a sequential Monte Carlo technique for detection and a subsequent information driven control of the observer for the purpose of parameter estimation of an unaccounted point source of relatively low-level gamma radiation. The search for nuclear materials in a similar context has been considered earlier in [7,9]. In [7], the authors apply a sequence of statistical hypothesis tests for a survey on a predetermined route. Our goal, however, is to perform an on-line feedback of detection and estimation results into the search plan and thus control the observer motion and the radiation exposure times. Another fundamental difference between our problem formulation and those presented in [7,9] is that we exploit prior knowledge of the propagation properties of gamma radiation, experimentally verified to obey the inverse distance square law.

The problem can be described informally as follows. Suppose that based on an intelligence report, an area has been identified where an unaccounted radiological source is likely to be found. Our goal is twofold. First, by searching the area, the presence of the source has to be firmly established (this is the detection part). Second, if the source has been detected, it has to be localised in an optimal manner (for example, by minimising the number of measurement acquisition steps, or by minimising the total search time). This second part involves both estimation and resource allocation strategies. Our study is restricted to the case where the point source, to be detected and localised, is static and placed in an open field.

* Corresponding author. Tel.: + 61 3 9626 8226; fax: +61 3 9626 8409.
E-mail address: branko.ristic@dsto.defence.gov.au (B. Ristic).

1566-2535/$ - see front matter Crown Copyright © 2007 Published by Elsevier B.V. All rights reserved.
doi:10.1016/j.inffus.2007.06.004

The paper is organised as follows. A formal problem description is presented in Section 2. Section 3 describes the conceptual solution based on the particle filter, for detection and estimation, and the information gain control of the observer. Section 4 details two versions of the particle filter. Section 5 is devoted to the observer control for the purpose of fast, accurate and safe estimation of the source parameters. The numerical simulation results are presented in Section 6 and the findings of this study are summarised in Section 7.

2. Problem formulation

Suppose an area has been identified in which the potential presence of a radiological point source has to be confirmed. For simplicity, let us assume that this area is flat and rectangular with limits $x_{\min}$ and $x_{\max}$ along axis x and similarly $y_{\min}$ and $y_{\max}$ along axis y.

Equipped with a radiation survey instrument, mounted on a vehicle or carried by a person, the task is to quickly confirm the presence of the source and in the case of positive detection, estimate its location and its level of radiation intensity. The radiological survey instrument typically consists of: (1) a sensor, a gamma radiation detector measuring dose-counts per second, (2) a differential GPS receiver, measuring own positions and (3) a computer, interfacing with the sensor/GPS receiver, performing data processing and displaying the control instructions and results. The movement of the radiation survey instrument is assumed to be constrained by the human factor, in the sense that a cumulative exposure to radiation should be kept at minimum. This constraint can be relaxed (e.g. if an unmanned vehicle is carrying the equipment) and others may be imposed (e.g. terrain) if required.

The radiation counts from nuclear decay obey Poisson statistics [23,9], as we experimentally verified in [4]: the probability that a gamma radiation detector registers $z \in \mathbb{Z}^+$ counts in τ seconds, from the source that emits on average μ counts per second is:

$$\mathscr{P}(z;\lambda) = \frac{\lambda^z}{z!}\mathrm{e}^{-\lambda}, \tag{1}$$

where $\lambda = \mu\tau$ is the parameter of the Poisson distribution. Both mean and the variance of random variable z are equal to λ.

The radiation source will be parameterized by:

- its location (x_s, y_s) in the Cartesian coordinate system, where $x_{\min} \leqslant x_s \leqslant x_{\max}$ and $y_{\min} \leqslant y_s \leqslant y_{\max}$;
- its equivalent intensity rate, $\mathscr{I}_s$, which is approximately given by the expression $M\varepsilon/6$, where M is the activity of the radioactive source, and ε is the gamma energy per disintegration [16]. Formally, we may assume that $\mathscr{I}_{\min} \leqslant \mathscr{I}_s \leqslant \mathscr{I}_{\max}$, although the values of $\mathscr{I}_{\min}$ and $\mathscr{I}_{\max}$ may not be known (in the case of complete ignorance $\mathscr{I}_{\min} = 0$ and $\mathscr{I}_{\max} \to \infty$).

Thus, the source parameter vector is given by:

$$\mathbf{x} = [x_s \quad y_s \quad \mathscr{I}_s]^{\mathrm{T}}, \tag{2}$$

where T denotes the matrix transpose.

Given the parameter vector $\mathbf{x}$, the likelihood function of a radiation count measurement z_k, registered at precisely known location (x_k, y_k), $k = 1, 2, \ldots$ during an exposure period of τ_k seconds, is given by:

$$p(z_k|\mathbf{x}) = \mathscr{P}(z_k; \lambda_k(\mathbf{x})) \tag{3}$$

where $\mathscr{P}$ is the Poisson distribution defined in (1), and

$$\lambda_k(\mathbf{x}) = \left[\frac{\mathscr{I}_s}{(x_k - x_s)^2 + (y_k - y_s)^2} + \mu_b\right]\tau_k \tag{4}$$

is the mean radiation count. The expression for λ_k above, valid for a point source emitting uniformly in all directions, is based on the inverse square distance law [16] (the distance is between the radioactive source and the sensor). In this context, $\mathscr{I}_s$ represents the average number of counts per second due to the source, recorded at a distance $d_k = \sqrt{(x_k - x_s)^2 + (y_k - y_s)^2}$ of 1 m from its location. The constant μ_b in (4) represents the mean count-rate of the background radiation, that is, the average number of counts per second when $\mathscr{I}_s = 0$ or when d_k is infinite.

3. Conceptual solution

Let us for a moment disregard the sensor control aspect of the problem (i.e. how the measurements of radiation intensity are collected). The goal is to jointly detect and estimate the source parameter vector using a cumulative set of recorded measurements. The problem has many similarities to the recursive track-before-detect described in [21, Chapter 11], except that the likelihood functions are different and, more importantly, here we treat the problem as a static parameter estimation problem. In order to perform detection, we introduce an additional binary random variable E, such that $E = 0$ if the source is absent and $E = 1$ if the source is present in the region. Joint detection and estimation is then treated as a hybrid (continuous-discrete) estimation problem.

In the recursive Bayesian framework, the hybrid estimation problem is formulated as follows. Let the joint posterior density of the source parameter vector and its presence/absence random variable, after processing k measurements, be denoted by $p(\mathbf{x}, E|Z_k)$, where $Z_k = \{z_1, \ldots, z_k\}$ is the accumulated set of measurements. Given a new $(k+1)$st measurement z_{k+1}, the goal is to construct the updated posterior density $p(\mathbf{x}, E|Z_{k+1})$ using the measurement model given by (3) and (4). For the case $E = 1$, this is done via:

$$p(\mathbf{x}, E = 1|Z_k) = \frac{p(z_k|\mathbf{x}, E = 1)p(\mathbf{x}, E = 1|Z_{k-1})}{p(z_k|Z_{k-1})} \tag{5}$$

For the case $E = 0$, the source state is not defined, hence we have:

$$p(E=0|Z_k)=\frac{p(z_k|E=0)p(E=0|Z_{k-1})}{p(z_k|Z_{k-1})}. \quad (6)$$

The likelihood function for the two cases of E, according to (3) and (4), is given by:

$$p(z_k|\mathbf{x},E=1)=\mathscr{P}(z_k;\lambda_k(\mathbf{x})) \quad (7)$$

$$p(z_k|E=0)=\mathscr{P}(z_k;\mu_b\tau_k) \quad (8)$$

Based on the posterior $p(\mathbf{x},E|Z_k)$, we can make inference about unknown random variables. For example, the posterior probability of source presence after processing k measurements:

$$P_k=\mathbb{P}\{E=1|Z_k\} \quad (9)$$

is computed as a marginal of $p(\mathbf{x},E=1|Z_k)$. Similarly, the mean of $p(\mathbf{x},E=1|Z_k)$ is the MMSE estimate of the parameter vector $\mathbf{x}$.

Next we can formulate the overall algorithm for detection and sensor controlled parameter estimation of a radiological source. Its main steps are shown in Table 1.

Steps 5.d and 5.f.(i.) refer to source detection and parameter estimation, captured by the posterior $p(\mathbf{x},E|Z_k)$. These two steps will be carried out jointly using a particle filter described in Section 4. The sensor control strategy (predefined versus optimised; where to move the sensor in order to collect the next measurement (in Step 5.b); how to choose the exposure time τ_k (in Step 5.c); and how to choose the search termination criterion in Step 5.h) will be discussed in Section 5.

4. Particle filter for integrated detection and estimation

The recursive Bayesian hybrid state estimator, which performs jointly detection and parameter estimation (Steps 5.d and 5.f.(i.)), is implemented as a particle filter (PF). The main idea of the PF is to represent the posterior distribution $p(\mathbf{x},E|Z_k)$ through a finite set of random samples (particles). When a new observation z_{k+1} is received, the particles are updated in order to represent the new posterior $p(\mathbf{x},E|Z_{k+1})$. An additional problem in our context is that both $\mathbf{x}$ and E are static parameters. It is well known that in this case after a few steps all particles will collapse to a single point (the sample impoverishment effect) [11,18]. In this paper we will increase the diversity of particles (and thus avoid the sample impoverishment) by simply adding a small amount of noise to the particles. The negative consequences of this technique (e.g. the most recent observation has the strongest influence on the the parameter estimate) will have a very small effect on the overall performance.

In this section we describe two particle filtering schemes, which both implement the described recursive Bayesian state estimator. The first PF is based on the augmented parameter vector consisting of the source parameters $\mathbf{x}$ and the existence variable E. The second PF is a Rao-Blackwellised version of the first, and does not require variable E in the state vector.

Table 1
Algorithm for detection and sensor controlled parameter estimation of a radiological source

(1) $k=0$
(2) Initialisation
(3) SEARCH = 'ON'
(4) CONTROL = 'PREDEFINED'
(5) **WHILE** SEARCH = 'ON'
  a. Increment k
  b. Move the sensor to a new location (x_k,y_k)
  c. Measure the number of counts z_k in τ_k seconds
  d. Determine the probability that the source is present P_k
  e. **IF** $P_k < P^*$ **THEN**
    (i.) CONTROL = 'PREDEFINED'
  f. **ELSE**
    (i.) Estimate the posterior $p(\mathbf{x},E|Z_k)$
    (ii.) CONTROL = 'OPTIMISED'
  g. **END IF**
  h. **IF** SEARCH-CRITERION satisfied
  i. SEARCH = 'OFF'
  j. **END IF**
(6) **END WHILE**

Variable definition: SEARCH ∈ {'ON','OFF'}, CONTROL ∈ {'PREDEFINED','OPTIMISED'}.

4.1. PF for augmented parameter vector

Let the augmented parameter vector be $\mathbf{y}=[\mathbf{x}^{\mathrm{T}}\ E]^{\mathrm{T}}$. The posterior pdf $p(\mathbf{y}|Z_k)$ is approximated by a finite set $\{\mathbf{y}_k^n,w_k^n\}_{n=1}^N$, where $\mathbf{y}_k^n$ is a particle consisting of $\mathbf{x}_k^n$ and E_k^n, w_k^n is a (normalised) particle weight and N is the number of particles. In step 2 of the algorithm in Table 1 (when $k=0$), the particles are initialised based on our prior knowledge as follows. A certain number N_p of particles is initialised as if the source is present: $E_0^n=1$, for $n=1,2,\ldots,N_p\ll N$. For those "source-existing" particles, we initialise the parameter vector components as:

$$x_0^n\sim\mathscr{U}[x_{\min},x_{\max}]$$
$$y_0^n\sim\mathscr{U}[y_{\min},y_{\max}]$$
$$\mathscr{I}_0^n\sim\mathscr{U}[\mathscr{I}_{\min},\mathscr{I}_{\max}]$$

for $n=1,\ldots,N_p$. The remaining particles are initialised with $E_0^n=0$, $n=N_p+1,\ldots,N$; their parameter vector components are not defined.

We adopt to implement the PF as the SIR filter [3,21], consisting of four steps in this particular order: computation of weights; resampling; diversity augmentation and the computation of the output.

Computation of weights. In the SIR filter the weights are proportional to the corresponding likelihood functions under each of the "source exists" hypotheses. Thus once a measurement z_k is collected, the importance weight of particle $\mathbf{y}_k^n$, $n=1,\ldots,N$ is

$$w_k^n\propto\begin{cases}\mathscr{P}(z_k;\lambda_k(\mathbf{x}_k^n)) & \text{if } E_k^n=1\\ \mathscr{P}(z_k;\mu_b\tau_k) & \text{if } E_k^n=0,\end{cases} \quad (10)$$

where the likelihood functions were defined in (7) and (8). In order to avoid the potential numerical problems it is more convenient to implement the computation of the weights using the likelihood ratio:

$$\ell(z_k|\mathbf{x}_k^n) = \frac{\mathscr{P}(z_k;\lambda_k(\mathbf{x}_k^n))}{\mathscr{P}(z_k;\mu_b\tau_k)} = \left(\frac{\lambda_k(\mathbf{x}_k^n)}{\mu_b\tau_k}\right)^z \cdot \exp\{\mu_b\tau_k - \lambda_k(\mathbf{x}_k^n)\}. \quad (11)$$

The unnormalised weights are then computed as:

$$\tilde{w}_k^n = \begin{cases} \ell(z_k|\mathbf{x}_k^n) & \text{if } E_k^n = 1 \\ 1.0 & \text{if } E_k^n = 0, \end{cases} \quad (12)$$

followed by the normalisation step: $w_k^n = \tilde{w}_k^n / \sum_{n=1}^N \tilde{w}_k^n$.

Resampling. The role of resampling is to eliminate the samples with low importance weights and to clone the samples with high importance weights. It involves a mapping of a random measure $\{\mathbf{y}_k^n, w_k^n\}_{n=1}^N$ into a new random measure $\{\mathbf{y}_k^{n*}, 1/N\}_{n=1}^N$, which has uniform weights. Several efficient resampling schemes have been reported in the literature, such as the stratified sampling [2], residual sampling [13] and systematic resampling [8]. We have implemented the systematic resampling algorithm, following the pseudo-code given in Table 3.2 of [21].

Augmentation of diversity. For each "existing" particle n (characterised by $E_k^{n*} = 1$), the value of $\mathbf{x}_k^{n*}$ is jittered via regularisation [3,12,18] with a Gaussian kernel. Let us denote the 3×3 empirical covariance matrix of the "existing" particles *before* resampling as:

$$\mathbf{S}_k = \mathrm{Cov}\{\mathbf{x}_k^n \text{ s.t. } E_k^n = 1\}_{n=1}^N. \quad (13)$$

Let $\mathbf{A}_k$ be the principal square root of $\mathbf{S}_k$, i.e.

$$\mathbf{A}_k\mathbf{A}_k^{\mathrm{T}} = \mathbf{S}_k. \quad (14)$$

Then jittering of an "existing" particle n is carried out as follows:

$$\mathbf{x}_k^{n*} := \mathbf{x}_k^{n*} + h\mathbf{A}_k\epsilon^n, \quad (15)$$

where ϵ^n is a Gaussian random vector of dimension 3 (with zero mean and variance one) and h is the "bandwidth" of the kernel [18].

Output. The probability that the source is present, defined by (9), is approximated as

$$P_k \approx \frac{1}{N}\sum_{n=1}^N E_k^{n*}. \quad (16)$$

The MMSE estimate of the source parameter vector is computed by:

$$\hat{\mathbf{x}}_k = \int \mathbf{x}p(\mathbf{x}, E=1|Z_k)\,\mathrm{d}\mathbf{x} \approx \frac{\sum_{n=1}^N \mathbf{x}_k^{n*}\cdot E_k^{n*}}{\sum_{n=1}^N E_k^{n*}} \quad (17)$$

if $P_k \geqslant P^*$, where P^* is the detection threshold.

An intuitive explanation of the PF mechanics is as follows. Suppose the value of z_k is very small. Then the "existing" particles of large intensity, located in the vicinity of the measurement location (x_k, y_k), will be assigned unnormalised weights smaller than 1, and most likely will be eliminated in the resampling step. On the contrary, if z_k is large, all "existing" particles will have a better chance of survival and, as a result, the probability P_k will increase. The number of particles here is fixed over time, but the ratio between the number of "existing" and "non-existing" particles is time varying and determines the probability P_k.

4.2. Rao-Blackwellisation

The described particle filter for hybrid state estimation can be implemented without an explicit need for variable E_k in the parameter vector of each particle. The idea is to keep only nominally a single $E_k = 0$ particle with a time-varying weight, while all N factual particles in the filter are representing the $E_k = 1$ hypothesis, see for example [22]. The particles in our case are therefore three-dimensional vectors $\mathbf{x}_k^n$, $n = 1, \ldots, N$.

Suppose that the weight corresponding to the "phantom" $E_k = 0$ particle is q_k. Since all factual particles in the filter are $E_k = 1$ particles, by adopting the "transitional prior" for the importance density [21, p. 47], their unnormalised weights are computed as follows:

$$\tilde{w}_k^n = \ell(z_k|\mathbf{x}_k^n)w_{k-1}^n \quad (18)$$

where w_{k-1}^n is the weight of particle n at time $k-1$, equal to:

$$w_{k-1}^n = (1-q_k)/N. \quad (19)$$

Eq. (19) reflects the fact that after the resampling step (at time $k-1$), the $E_k = 1$ particles have uniform weights. Taking into account the weight of the phantom particle, the weights are normalised as follows:

$$w_k^n = \frac{\tilde{w}_k^n}{\sum_{n=1}^N \tilde{w}_k^n + q_k} \quad (20)$$

After the resampling step we compute the new phantom particle weight as follows: $q_{k+1} = 1 - \sum_{n=1}^N w_k^n$.

In order to be compatible with the initialisation of particles in Section 4.1, initially we set $q_1 = (N - N_p)/N$, and from (19) follows that $w_0^n = N_p/N^2$, $n = 1, \ldots, N$. The probability that the source is present is then approximated as:

$$P_k \approx \sum_{n=1}^N w_k^n. \quad (21)$$

As before, the particles after resampling are denoted by $\mathbf{x}_k^{n*}$, and if $P_k \geqslant P^*$, the MMSE estimate of the source parameter vector is computed as:

$$\hat{\mathbf{x}}_k \approx \sum_{n=1}^N \mathbf{x}_k^{n*}. \quad (22)$$

5. Sensor control

The radiological survey instrument is controlled automatically for the purpose of detection and parameter estimation of a radioactive source. While P_k is below a certain threshold value P^*, in the absence of any prior information on the source location, the measurements are taken along a predefined path that scans the area in a uniform manner (known as the parallel sweeps search [10]). An example of a path scanning the area is shown in Fig. 1, where Δ is the distance between consecutive measurement locations. The choice of Δ depends on (unknown) $\mathscr{I}_s$ and is discussed in [26]. During this phase of the search, the exposure interval τ_k is kept constant.

The issues to consider in this first phase of the search are, for example: (1) the choice of the pair P^* and Δ and its relationship to the probability of detection and the probability of false alarm; (2) the efficiency of search by computing the exposure time in the sequential testing scheme described in [9]. The search-paths and detection aspects for this first phase are covered in the classical textbooks such as [10,25]. In this paper, however, we focus on the second phase of the search, when P_k exceeds the threshold. In this second phase, the algorithm controls the radiological survey instrument (i.e. chooses the next measurement location (x_{k+1}, y_{k+1}) and the exposure interval τ_{k+1}) in order to optimise the source parameter estimation. Somewhat similar problems have been considered in the bearings-only literature as observer motion strategies [6,15,20,1]. Having established that the focus of the paper is on the post-detection sensor control, in the remainder we will assume that the values of Δ and P^* are chosen so that the probability of detection and the probability of false alarm are practically one and zero, respectively.

5.1. Optimisation criterion

The next measurement location (x_{k+1}, y_{k+1}) and the exposure time τ_{k+1} are commonly referred to as the control parameters. We choose to select the control parameters in such a way that the measurement information gain (in the context of the Fisher information) is maximised, but at the same time the radiation exposure is not excessive.

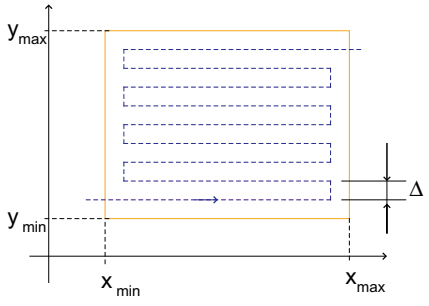

Fig. 1. Predetermined search pattern while $P_k < P^*$.

Next we explain how we compute the measurement contribution to the Fisher information matrix (FIM) at instant $k+1$, denoted by $\delta\mathbf{J}_{k+1}$. By definition [24, p. 80],

$$\delta\mathbf{J}_{k+1}(\mathbf{x}) = -\mathsf{E}[\nabla_{\mathbf{x}}\nabla_{\mathbf{x}}^{\mathrm{T}} \log p(z_{k+1}|\mathbf{x}, E=1)] \tag{23}$$

where E is the expectation operator with respect to the measurement, $\nabla_{\mathbf{x}}$ is the gradient operator with respect to $\mathbf{x}$ and $p(z_{k+1}|\mathbf{x},E=1)$ is the likelihood function given by (7).

Following the derivation in [17], we obtain the closed form solution:

$$\delta\mathbf{J}_{k+1}(\mathbf{x}) = \frac{\nabla_{\mathbf{x}}\lambda_{k+1}(\mathbf{x})\nabla_{\mathbf{x}}^{\mathrm{T}}\lambda_{k+1}(\mathbf{x})}{\lambda_{k+1}(\mathbf{x})} \tag{24}$$

Note that

$$\nabla_{\mathbf{x}}\lambda_k(\mathbf{x}) = \left[\frac{\partial\lambda_k(\mathbf{x})}{\partial x_s} \quad \frac{\partial\lambda_k(\mathbf{x})}{\partial y_s} \quad \frac{\partial\lambda_k(\mathbf{x})}{\partial\mathscr{I}_s}\right]^{\mathrm{T}} \tag{25}$$

and with the partial differentiation of (4) we obtain:

$$\frac{\partial\lambda_k}{\partial x_s} = \frac{2(x_k - x_s)\mathscr{I}_s\tau_k}{[(x_k-x_s)^2 + (y_k-y_s)^2]^2} \tag{26}$$

$$\frac{\partial\lambda_k}{\partial y_s} = \frac{2(y_k - y_s)\mathscr{I}_s\tau_k}{[(x_k-x_s)^2 + (y_k-y_s)^2]^2} \tag{27}$$

$$\frac{\partial\lambda_k}{\partial\mathscr{I}_s} = \frac{\tau_k}{(x_k-x_s)^2 + (y_k-y_s)^2}. \tag{28}$$

An obvious problem for the sequential (on-line) sensor control is that, in order to compute the FIM of (24), the source parameter vector $\mathbf{x}$ must be known. In the absence of $\mathbf{x}$ we have two choices: either replace $\mathbf{x}$ in (24) by its current estimate $\hat{\mathbf{x}}_k$ computed by the PF (using Eq. (17) or (22)), or compute $\delta\mathbf{J}_k(\mathbf{x}_k^n)$ for each particle and then find its mean value. The latter choice is computationally more demanding, but more reliable in situations where the posterior density $p(\mathbf{x}, Z_k)$ is multi-modal.

5.2. Optimisation strategy

Let us denote the control parameters by vector $\mathbf{u}_k = [x_k, y_k, \tau_k]^{\mathrm{T}}$, and similarly the control path from k to $s \geqslant k$ as $\mathbf{u}_{k,s} = [\mathbf{u}_k, \mathbf{u}_{k+1}, \ldots, \mathbf{u}_s]$. Ideally, the entire control path $\mathbf{u}_{k+1,\infty}$ should be selected at once based on the FIM computed at multiple (up to infinity) steps ahead, that is:

$$\mathbf{u}_{k+1,\infty} = \arg\max_{\mathbf{u}_{k+1,\infty}} \left[\mathrm{tr}\left\{\sum_{\ell=k+1}^{\infty} \delta\mathbf{J}_\ell(\mathbf{u}_\ell)\right\}\right] \tag{29}$$

where tr denotes the trace of a matrix and $\delta\mathbf{J}_\ell$ was defined by (24). There are, however, two practical problems that prevent us from using (29). First, for computational reasons, we have to restrict our search to only a few steps ahead procedure, due to the exponential growth in the number of possible control path options. Second, there is no point in looking too many steps ahead anyway, since in the computation of $\delta\mathbf{J}_\ell$, for $\ell = k+1, k+2, \ldots$, we rely on an uncertain estimate $\hat{\mathbf{x}}_k$ or the approximation of the

posterior $p(\mathbf{x}|Z_k)$ produced by the PF. The uncertainty about the true $\mathbf{x}$ is higher in the earlier stages of the search.

Based on these practical limitations, we have implemented a control vector optimisation procedure that looks up to L-steps ahead ($L>0$). In order to evaluate the FIM over the control vector space, we have discretised the $2L$-dimensional space of future sensor locations $(x_{k+\ell}, y_{k+\ell})$, $\ell = 1,\ldots,L$ in the following manner:

$$(x_{k+\ell}, y_{k+\ell}) \in \{(x_{k+\ell-1} + mD, y_{k+\ell-1} + nD); \\ m,n = -1,0,1; \ell = 1,\ldots,L\}, \tag{30}$$

where parameter D is the motion increment. In this way the number of considered future sensor locations for the evaluation of the FIM is 9^ℓ for an ℓ step-ahead search. The discretised values were selected as a compromise between the computational requirements (number of control paths to be evaluated) and the algorithm performance.

For each prospective sensor location we also need to assign the radiation exposure time $\tau_{k+\ell}$. Assuming that the radiation survey instrument is carried/operated by a human, we place a limit on the maximum allowed instantaneous radiation. Let us first define the signal-to-noise (SNR) ratio for a source. For this purpose we will approximate the Poisson distribution, parameterised by λ, with a Gaussian pdf of mean λ and standard deviation $\sqrt{\lambda}$, that is: $\mathscr{P}(z;\lambda) \approx \mathscr{N}(z;\lambda,\sqrt{\lambda})$. Then we can adopt the following measurement model:

$$z_k \approx \lambda_k(\mathbf{x}) + w_k \tag{31}$$

where w_k is additive zero-mean white Gaussian noise with variance $\lambda_k(\mathbf{x})$, defined by (4). The SNR is defined as the ratio of signal power (λ_k^2) to the noise power (λ_k), which in the log scale results in the following definition:

$$\mathrm{SNR}_k[\mathrm{dB}] \approx 10\log\lambda_k(\mathbf{x}). \tag{32}$$

Here we make a similar remark to the one at the end of Section 5.1: in the computation of $\lambda_k(\mathbf{x})$ in (32) we can either use the current point estimate $\hat{\mathbf{x}}_k$ or the average over the particles.

We do not want at any point of time the SNR value to exceed a predefined SNR threshold γ. Then for each prospective sensor location $(x_{k+\ell}, y_{k+\ell})$, we assign the exposure time $\tau_{k+\ell}$ that correspond to γ, using the current source parameter vector estimate $\hat{\mathbf{x}}_k = [\hat{x}_s \hat{y}_s \hat{\mathbf{I}}_s]^{\mathrm{T}}$. From (4) and (32) it follows then:

$$\tau_{k+\ell} = \left\lceil 10^{\gamma/10} \cdot \left(\frac{\hat{\mathbf{I}}_s}{(x_{k+\ell}-\hat{x}_s)^2 + (y_{k+\ell}-\hat{y}_s)^2} + \mu_b \right)^{-1} \right\rceil \tag{33}$$

When we search for a multi-step ahead control path $\mathbf{u}_{k+1,\ldots,k+L}$, we predict the SNR value at the closest point of approach to the source for all control vectors $\mathbf{u}_{k+1}$ to $\mathbf{u}_{k+L}$ in the path, using the current source estimate $\hat{\mathbf{x}}_k$. If for any of them the SNR value exceeds γ, we discard the entire multi-step ahead control path as being unacceptably dangerous.

Once we select the next control vector $\mathbf{u}_{k+1}$, we acquire measurement z_{k+1} and then (using the PF) we compute the new estimate of the posterior pdf $p(x,E|Z_{k+1})$, and subsequently P_{k+1} and $\hat{\mathbf{x}}_{k+1}$. Then we check if the SNR (using the new estimate $\hat{\mathbf{x}}_{k+1}$) is less than γ. If yes, we immediately direct the survey instrument to be moved radially away from the estimated source location until the SNR falls below the threshold γ. Next, we search for the new multi-step ahead control path $\mathbf{u}_{k+2,\ldots,k+L+1}$, using the current source estimate $\hat{\mathbf{x}}_{k+1}$, and so on.

5.3. Algorithm termination criterion

There are two termination criteria. For the search along the predefined control path (i.e. while $P_k < P^*$), the search continues until the entire observer path is traversed or if the probability P_k falls to zero. During the information gain driven observer control (i.e. while $P_k \geqslant P^*$), the algorithm is terminated if:

$$\mathrm{tr}\{\mathbf{A}_k\} < \eta, \tag{34}$$

where $\mathbf{A}_k$ was defined in (14). This termination criterion states that the search is completed when the spread of the "existing" particles is below a certain threshold η.

6. Numerical results

6.1. Simulation parameters

A radiological point source of an equivalent intensity $I_s = 18\times10^3$ cts/s is placed at $x_s = 240$ m, $y_s = 532$ m in a 2D Cartesian plane. Our prior knowledge is as follows: $x_{\min} = 100$ m, $x_{\max} = 600$ m, $y_{\min} = 300$ m, $y_{\max} = 800$ m, $I_{\min} = 8\times10^3$ cts/s and $I_{\max} = 33\times10^3$ cts/s. The mean count-rate of the background radiation is $\mu_b = 1$ cts/s. The count measurements were generated using a Poisson random number generator and the propagation model (4).

The parameters of the proposed algorithm are: $N_p = N/10$, $N = 30{,}000$, $h = 0.005$, $P^* = 0.75$, $\Delta = 50$ m, $D = 0.75\Delta$, $\eta = 100\Delta$. The exposure time when $P_k < P^*$ is fixed at $\tau_k = 4$ s. Finally, the danger SNR threshold γ is set to 12 dB.

6.2. Single run results

First we illustrate a typical run of the algorithm with $L = 2$ step-ahead observer control optimisation, using Rao-Blacwellised PF with the FIM gain computed as $\frac{1}{N}\sum_{n=1}^{N}\delta\mathbf{J}_k(\mathbf{x}_k^n)$. Fig. 2 shows the observer path with spread of particles at six characteristic time steps. Fig. 3 displays the time evolution of z_k, P_k and τ_k for this run, while Fig. 4 plots the final histogram of particles in $\mathscr{I}_s$ space.

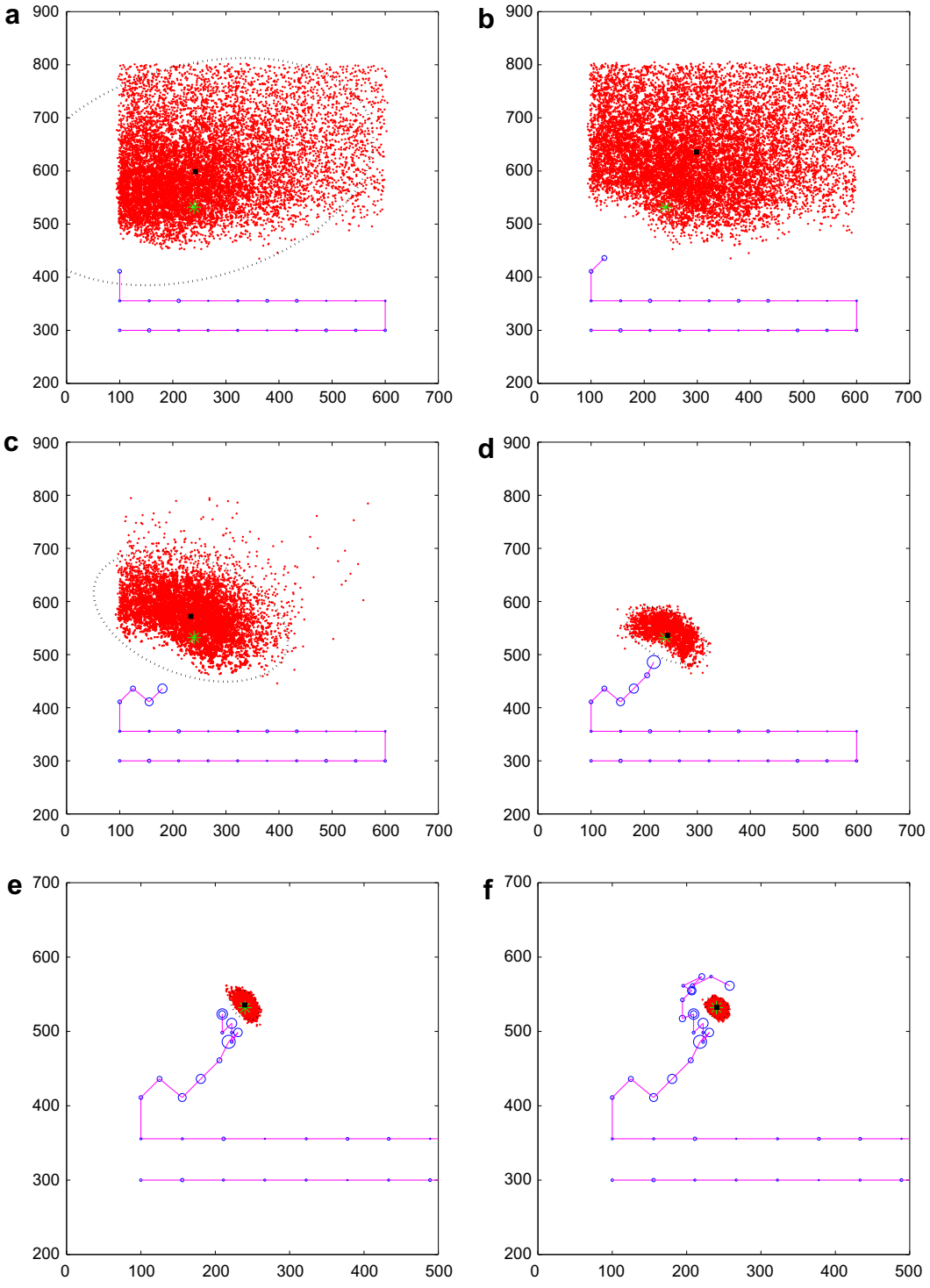

Fig. 2. Source localisation after processing: (a) $k = 21$, (b) $k = 22$, (c) $k = 24$, (d) $k = 26$, (e) $k = 33$, (f) $k = 43$ measurements (figures (e) and (f) are zoomed in).

At first the search follows the predetermined path (magenta line) with τ_k fixed at 4s. Blue circles[1] are centered at (x_k, y_k) and their diameter corresponds to the size of the measurement z_k. The presence of the source is established after processing $k = 21$ measurements, since at this point probability $P_{21} \geqslant P^*$ (see Figs. 2a and 3b). The red dots[1] in Fig. 2a indicate the positions of particles after resampling at $k = 21$. Observe how the region which has been

[1] For interpretation of color in Figs. 2 and 4, the reader is referred to the web version of this article.

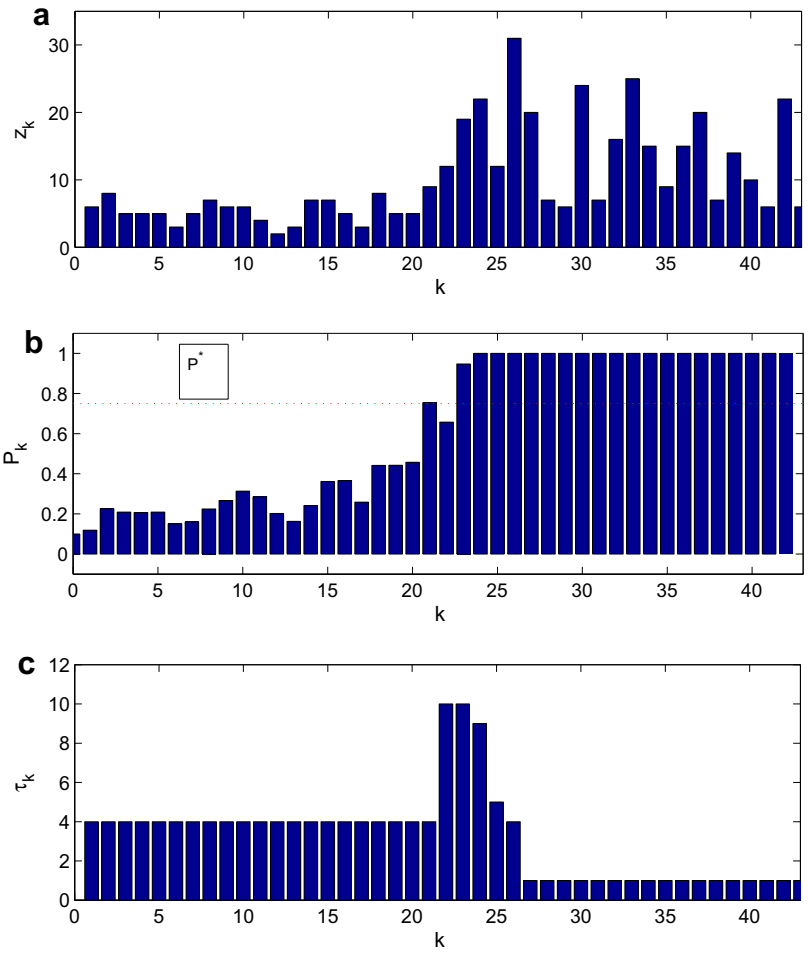

Fig. 3. Time evolution of: (a) measurements z_k, (b) probability P_k, (c) exposure time τ_k in seconds.

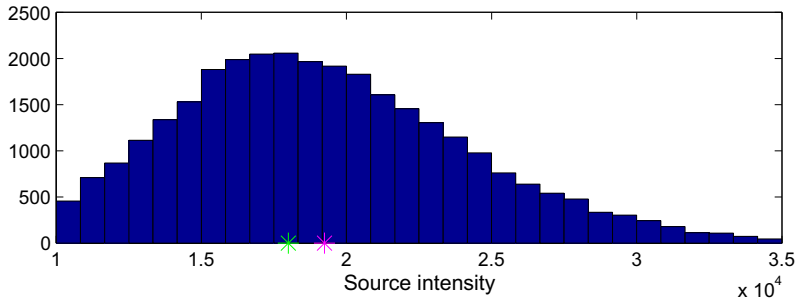

Fig. 4. The histogram of particles in the source intensity component after processing all 43 measurements (the true value is $\mathscr{I}_s = 1.8 \times 10^4$ cts/s).

traversed by the observer contains no particles, because the algorithm at this stage established that this region does not contain the radiological source. Note also that the particles are not placed outside the region limited by $x_{\min}$, $x_{\max}$, $y_{\min}$ and $y_{\max}$. The black square in Fig. 2 indicates the mean of the particle cloud, while the *3*-sigma uncertainty ellipse is shown in a dashed black line. The true source location is marked by the green asterisk.[1]

The observer is controlled to move towards the source at $k = 22$, with a large exposure time of *10*s. However, the received measurement z_{22} happened to be smaller than expected and the probability P_{22} dropped below the threshold P^*. The next two measurements, however, are very large and from $k = 23$ onwards, the source existence is firmly confirmed. The algorithm has decided to move towards the source until $k = 26$, with large exposure times, see Figs. 2d and 3c. This resulted in larger count measurements which culminated with $z_{26} = 32$, see Fig. 3a. Note from Fig. 2 how the spread of particles reduces from one step to the next. The termination criterion, however, has

not been satisfied at $k = 26$ and the algorithm continues to collect more measurements until $k = 43$, albeit with a small exposure time of *1*s. Note from Fig. 2e that, after approaching very close to the source at $k = 26$, the observer starts to follow a trajectory around the source, with occasional moves away from it. These moves away from the source are due to the estimated SNR exceeding the danger threshold γ. Also note that at $k = 32$ and $k = 33$ the observer stayed at the same location. At this point, the algorithm has decided that it needs a better estimate of source intensity and the observer was tasked to remained static. Fig. 2f shows the entire observer trajectory up to $k = 43$. The observer motion pattern is typical: the observer is at first approaching the source with large exposure times; once the observer is close to the source it then roughly follows a circular motion around the (estimated) source location, with a minimal exposure time. The observer trajectory is somewhat similar to optimal observer path when localising a static target with bearings only measurements [14,5]. Note however an important difference: in our problem there is an additional aspect of uncertainty due to the unknown source intensity.

An important property of the algorithm is that the true source location is always inside the 3σ uncertainty ellipsoids (see Fig. 2).

Fig. 4 shows the histogram of particles in $\mathscr{I}_s$ space, after processing all 43 measurements. The true source intensity is indicated by the green asterisk,[1] while the pink asterisk[1] corresponds to the mean of particles. In general, the errors in $\mathscr{I}_s$ space are fairly high, as predicted by the theoretical Cramér–Rao analysis[2] carried out in [4].

6.3. Monte Carlo runs

We run Monte Carlo (MC) simulations in order to establish the expected performance of different versions of the proposed algorithm. This is not a straightforward task, because, once the source is detected, the motion of the observer, the number of measurement steps, and the measurement values are different in each run.

We choose to compare the algorithms by MC runs in the following manner. For each MC run, we feed each of the contesting algorithms with identical pre-detection collected measurements (taken along the predefined path). In each run, of course, the pre-detection measurements are different, being Poisson distributed. We estimate the following set of *post-detection* performance measures, for each of the contesting algorithms:

Average number of measurement steps, defined as $\overline{K} = \frac{1}{C}\sum_{c=1}^{C}(K_{\mathrm{t}}^{c} - K_{\mathrm{d}}^{c})$, where K_{t}^{c} and K_{d}^{c} denote the number of observer steps in a Monte Carlo run $c = 1, \ldots, C$. Here K_{t}^{c} stands for the total number of steps, while K_{d}^{c} for the number of pre-detection steps.

Average accumulated exposure time, defined as $\overline{T} = \frac{1}{C}\sum_{c=1}^{C} T_c$, where $T_c = \sum_{k=K_{\mathrm{d}}^{c}+1}^{K_{\mathrm{t}}^{c}} \tau_k^c$ is the accumulated post-detection exposure time in a run c.

Average accumulated radiation count, defined as $\overline{Z} = \frac{1}{C}\sum_{c=1}^{C} Z_c$, where $Z_c = \sum_{k=K_{\mathrm{d}}^{c}+1}^{K_{\mathrm{t}}^{c}} z_k^c$ is the accumulated post-detection radiation count in run c.

RMS errors. Suppose the final estimate of the source parameter vector in run c is $\hat{\mathbf{x}}^c = [\hat{x}_s^c, \hat{y}_s^c, \hat{\mathscr{I}}_s^c]$. The RMS errors in the source position and intensity are defined as:

$$\rho_{\mathrm{p}} = \sqrt{\frac{1}{C}\sum_{c=1}^{C}(x_s - \hat{x}_s^c)^2 + \frac{1}{C}\sum_{c=1}^{C}(y_s - \hat{y}_s^c)^2}, \tag{35}$$

$$\rho_{\mathrm{i}} = \sqrt{\frac{1}{C}\sum_{c=1}^{C}(\mathscr{I}_s - \hat{\mathscr{I}}_s^c)^2} \tag{36}$$

respectively.

The first set of results, shown in Table 2, compares the particle filters of Sections 4.1 and 4.2, referred to as PF1 and PF2, respectively. The observer control in both PFs was carried out using $L = 1$ step ahead optimisation. The number of MC runs was $C = 25$. We observe from Table 2 that for $N = 10{,}000$ particles, the PF1 terminates quicker (in less steps) but with a much higher estimation error. For $N = 50{,}000$, both PFs achieve similar RMS estimation errors, but the PF2 is quicker (requires less steps, with a shorter exposure time and a smaller accumulated radiation count). The results can be explained by the fact that PF1 uses a smaller number of particles that are useful for estimation, than the PF2. Due to the termination criterion based on the spread of particles, when N is small, PF1 terminates quicker with a larger error. For large N, PF2 localises the source quicker because at the time of detection it has at its disposal a larger number of useful particles for estimation.

The second set of results, shown in Table 3, investigates the influence of the depths L in the control path optimisation, described in Section 5.2. The number of particles was $N = 40{,}000$, the number of MC runs $C = 25$. Since the termination criterion is the same in all cases, the final RMS errors are very similar. Using more than one-step ahead optimisation of control paths (at the cost of an increase in the computational load), reduces the number of observer steps and thus speeds up localisation. Note however the "diminishing returns" property of using the higher values of L: it appears that the three steps ahead procedure does

Table 2
The effect of Rao-Blackwellisation

	$\overline{K}$	$\overline{T}$ (s)	$\overline{Z}$ (cnts)	ρ_p (m)	ρ_i
Number of particles, $N = 10{,}000$					
PF1	22.48	39.44	263.64	34.84	6195.87
PF2	25.28	42.44	296.96	16.86	6555.59
Number of particles, $N = 50{,}000$					
PF1	39.72	68.12	450.72	8.05	5144.93
PF2	29.64	56.88	309.44	7.78	6064.19

[2] The Cramér–Rao (CR) analysis predicts the best achievable second-order error performance of an unbiased estimator. In order to compute the CR bound, one must know in advance the source parameters.

Table 3
The effect of the depth L in the control path optimisation

	$\overline{K}$	$\overline{T}$ (s)	$\overline{Z}$ (cnts)	ρ_p (m)	ρ_i
$L = 1$ step ahead	34.72	55.32	414.16	10.11	5808.84
$L = 2$ step ahead	27.72	50.16	292.12	9.70	5950.15
$L = 3$ step ahead	28.44	50.64	305.64	8.08	5377.01

not significantly improve the performance of the algorithm in comparison with the two-steps ahead optimisation.

7. Summary

The paper presented an algorithm for joint detection and parameter estimation of a radiological point source, where the emphasis was on post-detection observer control by maximisation of the Fisher information gain. The numerical simulations show a remarkably good performance of the algorithm under various conditions in the open field environment. There are many possibilities for future research and improvements of the basic algorithm described in this paper. First, a more efficient optimisation algorithm for multiple step ahead selection of the optimal control vector could be investigated. Second, a coordinated search using multiple networked observers in the presence of possibly multiple moving sources in the region of interest would be of practical interest. Finally, for a search in an urban environment, it would be necessary to exploit prior knowledge of obstacles and constraints that may affect both the gamma ray propagation and the selection of control parameters.

Acknowledgments

The authors thank the anonymous reviewers for valuable comments and Mark Rutten (DSTO) and Mark Morelande (The University of Melbourne) for useful technical discussions.

References

[1] J.P. Le Cadre, S. Laurent-Michel, Optimising the receiver maneuvers for bearings-only tracking, Automatica 35 (1999) 591–606.
[2] J. Carpenter, P. Clifford, P. Fearnhead, Improved particle filter for non-linear problems, IEE Proc. F 146 (1) (1999) 2–7.
[3] N.J. Gordon, D.J. Salmond, A.F.M. Smith, Novel approach to nonlinear/non-Gaussian Bayesian state estimation, IEE Proc. F 140 (2) (1993) 107–113.
[4] A. Gunatilaka, B. Ristic, R. Gailis, On localisation of a radiological point source, in: Proceedings of the Information, Decision and Control (IDC), Adelaide, Australia, February, 2007.
[5] S.E. Hammel, P.T. Liu, E.J. Hilliard, K.F. Gong, Optimal observer motion for localisation with bearings measurements, Comput. Math. Appl. 18 (1-3) (1989) 171–180.
[6] J.P. Helferty, D.R. Mudgett. Optimal observer trajectories for bearings-only tracking by minimizing the trace of the Cramér–Rao lower bound, in: Proceedings of 32nd IEEE Conference on Decision and Control, 1993, pp. 936–939.
[7] T. Hjerpe, R.R. Finck, C. Samuelsson, Statistical data evaluation in mobile gamma spectrometry: an optimisation of on-line search strategies in the scenario of lost point sources, Health Phys. 80 (6) (2001) 563–570.
[8] G. Kitagawa, Monte Carlo filter and smoother for non-Gaussian non-linear state space models, J. Comput. Graphical Stat. 5 (1) (1996) 1–25.
[9] A.V. Klimenko, W.C. Priedhorsky, N.W. Hengartner, K.N. Borozin, Efficient strategies for low-level nuclear searches, IEEE Trans. Nucl. Sci. 53 (3) (2006) 1435–1442.
[10] B.O. Koopman, Search and Scanning, Pergamon Press, 1980.
[11] D.S. Lee, N.K.K. Chia, A particle algorithm for sequential Bayesian parameter estimation and model selection, IEEE Trans. Signal Process. 50 (2) (2002) 326–336.
[12] J. Liu, M. West, Combined parameter and state estimation in simulation-based filtering, in: A. Doucet, J.F.G. de Freitas, N.J. Gordon (Eds.), Sequential Monte Carlo Methods in Practice, Springer, New York, 2001.
[13] J.S. Liu, R. Chen, Sequential Monte Carlo methods for dynamical systems, J. Am. Stat. Assoc. 93 (1998) 1032–1044.
[14] P.T. Liu, An optimum approach in target tracking with bearings measurements, J. Optim. Theory Appl. 56 (2) (1988) 205–214.
[15] A. Logothetis, A. Isaksson, R. Evans. Comparison of suboptimal strategies for optimal own-ship maneuvers in bearings-only tracking, in: Proc. Amer. Control Conf., Philadelphia, PA, USA, June, 1998, pp. 3334–3338.
[16] A. Martin, S.A. Harbison, An Introduction to Radiation Protection, Chapman & Hall, 1987.
[17] M. Morelande, B. Ristic, A. Gunatilaka, Detection and parameter estimation of multiple radioactive sources, in: Proc. 10th Int. Conf. Information Fusion, Quebec, Canada, July, 2007.
[18] C. Musso, N. Oudjane, F. LeGland, Improving regularised particle filters, in: A. Doucet, N. deFreitas, N.J. Gordon (Eds.), Sequential Monte Carlo methods in Practice, Springer, New York, 2001.
[19] W.K.H. Panofsky, Nuclear proliferation risks, new and old, Issues Sci. Technol. 19 (2003). Available from: http://www.issues.org/19.4/panofsky.html .
[20] J.M. Passerieux, D. Van Cappel, Optimal observer maneuver for bearings-only tracking, IEEE Trans. Aerospace Electron. Syst. 34 (3) (1998) 777–788.
[21] B. Ristic, S. Arulampalam, N. Gordon, Beyond the Kalman Filter: Particle Filters for Tracking Applications, Artech House, 2004.
[22] M.G. Rutten, N.J. Gordon, S. Maskell, Recursive track-before-detect with target amplitude fluctuations, IEE Proc. Radar Sonar Navig 152 (5) (2005) 345–352.
[23] N. Tsoulfanidis, Measurement and Detection of Radiation, Taylor & Francis, Washington, DC, 1995.
[24] H.L. VanTrees, Detection, Estimation and Modulation Theory (Part I), Wiley, 1968.
[25] A.R. Washburn, Search and Detection, fourth ed., Informs, 2002.
[26] K.P. Ziock, W.H. Goldstein, The lost source, varying backgrounds and why bigger may not be better, in: J.I. Trombka, D.P. Spears, P.H. Solomon (Eds.), Unattended Radiation Sensor Systems for Remote Applications, CP632, American Institute of Physics, 2002.